PAPR Reduction in MIMO-OFDM Systems Using Low-Complexity Additive Signal Mixing

Stephen Kiambi, Elijah Mwangi, and George Kamucha
School of Engineering, University of Nairobi, Kenya
Email: skiambi@uonbi.ac.ke; elijah.mwangi@uonbi.ac.ke; gkamucha@uonbi.ac.ke

Abstract—A MIMO-OFDM wireless communication technique possesses several advantages accrued from combining MIMO and OFDM techniques such as increased channel capacity and improved BER performance. This has made the technique very amiable to current and future generations of communication systems for high data-rate transmission. However, the technique also inherits the high PAPR problem associated with OFDM signals—a problem still requiring a practical solution. This work proposes a PAPR reduction algorithm for solving the problem of high PAPR in MIMO-OFDM systems. The proposed method uses a low-complexity signal mixing concept to combine the original transmit signal and a generated peak-cancelling signal. The computational complexity of the proposed method is $O(M)$, which is very much less than $O(N \log_2 N)$ of the FFT algorithms. This is because M, which denotes the number of nonzero peak-cancelling samples, is much less than N, the FFT window size. The proposed method was found to achieve high PAPR reductions while utilizing only a few nonzero peak-cancelling samples and it does not significantly change the power of the transmitted signal. For example, with $M = 5\%$ of 256-point IFFT samples, corresponding to a data rate loss of 4.8%, a large PAPR reduction of 5.9 dB could be achieved at a small power loss of 0.09 dB. Compared with other methods proposed in literature, the proposed method was found to outperform them in terms of PAPR reductions and BER performance.

Index Terms—High power amplifier, peak-to-average power ratio, multiple-input multiple-output, orthogonal frequency division multiplexing

I. Introduction

MIMO-OFDM, as the name suggests, is a technology that takes advantage of the benefits accruing from both Multiple-Input Multiple-Output (MIMO) communication and Orthogonal Frequency Division Multiplexing (OFDM) transmission to increase both data rate and reliability in in a communication system. On one hand, MIMO as a multiple-antenna technique in which multiple antennas are employed at both the transmitter and receiver can be used to bring in spatial diversity and/or spatial multiplexing to, respectively, boost the system reliability i.e. bit-error rate (BER), and increase the achievable data rate by the communication system. In addition, MIMO can also be used for beamforming, to increase coverage, and to reduce transmit power [1]. On the other hand, OFDM as a multicarrier modulation technique that employs parallel subcarriers to carry user data benefits the MIMO-OFDM communication system mainly with high transmission rates, high spectral efficiency, and the suppression of Inter-Symbol Interference (ISI).

The high spectral efficiency in OFDM is achieved by having all the parallel subcarriers mutually orthogonal to one another. The ISI is eliminated by using a combination of a symbol duration, which is much larger than the expected channel delay spread, and a guard interval between symbols that is simply larger than the delay spread. In addition, in every OFDM symbol, each subcarrier is equivalent to a subchannel. The number of subcarriers is chosen to ensure that each subchannel has a bandwidth less than the coherence bandwidth of the channel so that each of the subchannels experiences a relatively flat fading and therefore at the receiver only a simple single-tap equalizer is required to recover the transmitted data.

The several advantages outlined above have made MIMO-OFDM the key technology for the current and next generations of IEEE 802.16-based worldwide-interoperability for microwave access (WiMAX), 4G and 5G cellular networks, IEEE 802.11-based wireless LAN, wireless Personal Area Network, and broadcasting standards (Digital Audio Broadcasting (DAB), Digital Video Broadcasting (DVB), and Digital Multimedia Broadcasting (DMB)) [1].

Unfortunately, although all MIMO-OFDM systems have all the good attributes of OFDM, they also suffer from the drawbacks they inherit from OFDM. One of the major drawbacks of OFDM, and which is also passed to MIMO-OFDM, is the high peak-to-average power ratio (PAPR) that can occur in the transmit signal. The high PAPR can especially be at unacceptable levels when quite a substantial number or all of the modulated signals on the OFDM subchannels add constructively in a system with a large number of subcarriers. The processing in the High Power Amplifier (HPA) of such high PAPR signals will result to two nonlinear amplification effects, which are BER degradation and out-of-band radiations [2].

In order to avoid the two nonlinear amplification effects and therefore achieve distortionless processing of the high PAPR signals, a simple solution is to input back-off the HPA to a linear region far away from the 1-dB compression point. However, the input backed-off HPA

Manuscript received April 22, 2021; revised October 18, 2021.
Corresponding author email: skiambi@uonbi.ac.ke
doi:10.12720/jcm.16.11.468-478

will have low power efficiency and thus consume more input DC power. This will in turn reduce the lifetime of battery power at user terminals and increase the cost of the transmitter [3]. It is therefore more preferable to reduce any high PAPR in OFDM signals to suitable levels before the signals are passed to the HPA.

In the recent past, different methods have been proposed for PAPR reduction in OFDM and MIMO-OFDM systems. These include signal clipping [4], [5], companding [6], selective mapping [7], [8], partial transmit sequence [9], tone reservation [10], [11], hybrid schemes [12]-[14], etc. As can be noted, the majority of the methods proposed for use in OFDM systems can be re-designed to make them applicable in MIMO-OFDM systems. The proposed methods can generally be classified into four main categories [15]. These are signal distortion techniques, multiple-signalling and probabilistic techniques, coding techniques and hybrid techniques.

Under the signal distortion category, the methods reduce PAPR by distorting the signal before passing it to the HPA. In the multiple-signalling and probabilistic class, the methods both generate numerous alternatives of the OFDM signal and transmit the one with minimum PAPR or they reduce PAPR by modifying the OFDM signal through introduction of phase shifts, or addition of peak reduction tones, or alteration of constellation points. For the coding category, the methods choose the codewords that yield the minimum PAPR while the hybrid class utilises the advantages of different individual techniques and combine two or more schemes to improve PAPR reduction. For all the methods, the bottom line is to achieve significant PAPR reductions and improved BER performance at a minimal change in system complexity.

One of the simplest signal distortion technique employed to reduce PAPR is amplitude clipping, which is normally referred to as conventional clipping. However, the clipping operation can lead to severe BER degradation and high out-of-band radiations. An Adaptive Clipping Technique (ACT) attempting to overcome the shortcomings of the conventional clipping was proposed [16] for Alamouti space-time block code (STBC) MIMO-OFDM systems. However, even with the adaptive clipping, PAPR reductions had to be limited to avoid high BER degradation. In [17], a hybrid technique SCS-SLM combining Selective Codeword Shift (SCS) and selective mapping (SLM) schemes, with the aim of improving PAPR reduction, was proposed for STBC-based MIMO-OFDM systems. Although the hybrid scheme gave better performance than the individual SCS and SLM schemes, the PAPR reduction was still poor. Another hybrid PAPR reduction scheme CSC combining and optimizing three methods, namely convolutional code, successive sub-optimal cross-antenna rotation and inversion, and iterative modified companding and filtering was proposed for STBC-based MIMO-OFDM systems [18]. This method could significantly reduce PAPR but at the expense of poor BER performance and increased system complexity.

PAPR reduction methods that alter the original transmit signal by adding a peak-cancelling signal have been found the most promising because they can achieve both high PAPR reduction and improved BER performance [19]. Examples are methods based on tone reservations, where a subset of data subcarriers are reserved for carrying peak reduction coefficients which on Fourier transformation give the peak-cancelling signal. However, the tone reservation based methods suffer from three major drawbacks: the hard problem of finding the peak-reduction coefficients especially for optimal schemes, data rate loss, and increased transmit power. A sub-optimal Selective Tone Reservation (STR) method [20] was proposed for reducing PAPR in Space-Frequency Block Code (SFBC) MIMO-OFDM systems. The proposed algorithm is based on a time domain kernel, which is added to the signal of the antenna with maximum PAPR to reduce its peak power. Although the method had low complexity compared with an optimal scheme, it was prone to peak re-growth, increased transmit power and had poor PAPR reduction performance.

To overcome the drawbacks in tone reservation methods, in this paper, we propose a low-complexity additive signal mixing method for reducing PAPR in space-time-coded MIMO-OFDM systems. The key idea is to generate a peak-cancelling signal for each MIMO-OFDM branch based on a predetermined clipping threshold for the system at hand. To reduce PAPR, the respective peak-cancelling signals are added to the branch signals. For mitigating the data rate loss and the increase in the average power, only the nonzero samples of the peak-cancelling signals are transmitted together with the PAPR-reduced signals for use to reconstruct clipped amplitudes. In comparison with ACT, SCS-SLM, CSC, and S-TR methods, the proposed method was found to have better performance in PAPR reduction and BER improvement.

The rest of this paper is organized as follows. Section 2 presents the space-time block-coded MIMO-OFDM system and the associated PAPR. In Section 4, the proposed PAPR reduction method is presented. Section 5 provides simulation results and their analysis. Lastly, Section 6 concludes the paper.

II. MIMO-OFDM System and PAPR

A. Space-Time Block Code (STBC)

The very first and well-known STBC that provides transmit diversity is the Alamouti space-time code. The Alamouti code is a complex orthogonal space-time code specialised for the case of two transmit antennas but can be generalised to the case of three antennas or more. In the Alamouti encoder, two consecutive symbols X_1 and X_2 are encoded with the following space-time codeword matrix [21]:

$$X = \begin{bmatrix} X_1 & -X_2^* \\ X_2 & X_1^* \end{bmatrix} \quad (1)$$

where the $*$ denotes complex conjugate.

The Alamouti encoded signal is transmitted from the two transmit antennas over two symbol periods. During the first symbol period, the two symbols X_1 and X_2 are simultaneously transmitted from the first and the second antenna, respectively. In the second symbol duration, the same symbols are essentially re-transmitted in the form of two symbols, $-X_2^*$ and X_1^*, which are simultaneously transmitted from the first and the second antenna, respectively. At the receiver, an Alamouti STBC decoder is implemented.

Systems deploying multiple antenna techniques at the transmitter and the receiver are normally referred by their number of transmit and receive antenna configurations. There are two common implementations of Alamouti STBC receivers: one with one receive antenna and the other with two receive antennas corresponding to 2×1 and 2×2 systems, respectively. The two antenna configurations have the same channel capacity but different spatial diversity gains.

In general, the use of multiple antenna configurations in the transmitter and the receiver is supposed to increase the channel capacity of a single-input single-output (SISO) antenna configuration by a factor of $\min(N_t, N_r)$, where N_t and N_r are the number of transmit and receive antennas, respectively [22]. Since for the Alamouti STBC system, the same symbols are transmitted during two symbol durations, the channel capacity is still equal to the SISO system capacity. However, the Alamouti schemes achieve a diversity gain $N_d = N_t \times N_r$, which by definition is the number of independent channel paths between the transmitter and the receiver. The 2×2 antenna system has a diversity gain of four, which is double that of the 2×1 antenna system.

Since the probability of all the N_d channel paths having low signal-to-noise ratio (SNR) is very small, the diversity gain has profound effect on the system reliability. The average bit-error probability, p_b, of a multiple-antenna system decreases exponentially with the diversity gain [23] according to

$$p_b = k\Upsilon^{-N_d} \tag{2}$$

where k is a constant that depends on the modulation type and Υ is the received SNR. From this equation, it is clear that a 2×2 MIMO system offers a better BER performance than a multiple-input single-output (MISO) 2×1 system.

The Alamouti scheme for the 2×2 system is illustrated in Fig. 1. The channel impulse responses h_{11}, h_{12}, $h_{21}$and h_{22} are assumed to be time-invariant over two symbol durations and are of the form $|h_{ij}|e^{\theta_{ij}}$, where $|h_{ij}|$ and $e^{\theta_{ij}}$ denote the amplitude gain and phase alteration over the two symbol periods, and i and j are equal to 1 or 2.

The received signals at the first receive antenna (the upper receive antenna in Fig. 1) during the first and second symbol durations are, respectively, given by

$$\begin{aligned} Y_{11} &= h_{11}X_1 + h_{12}X_2 + n_{11} \\ Y_{12} &= -h_{11}X_2^* + h_{12}X_1^* + n_{12}. \end{aligned} \tag{3}$$

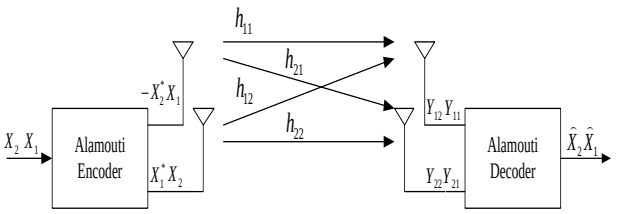

Fig. 1. Alamouti scheme for 2×2 MIMO system.

At the second antenna the received signals for the two symbol durations are:

$$\begin{aligned} Y_{21} &= h_{21}X_1 + h_{22}X_2 + n_{21} \\ Y_{22} &= -h_{21}X_2^* + h_{22}X_1^* + n_{22}. \end{aligned} \tag{4}$$

The four additive terms n_{11}, n_{12}, n_{21} and n_{22} in (3) and (4) represent additive white Gaussian noise. Taking the complex conjugate of the signals received during the second symbol duration, the system equation for the space-time-coded MIMO system can be written as follows:

$$\begin{bmatrix} Y_{11} \\ Y_{12}^* \\ Y_{21} \\ Y_{22}^* \end{bmatrix} = \begin{bmatrix} h_{11} & h_{12} \\ h_{12}^* & -h_{11}^* \\ h_{21} & h_{22} \\ h_{22}^* & -h_{21}^* \end{bmatrix} \begin{bmatrix} X_1 \\ X_2 \end{bmatrix} + \begin{bmatrix} n_{11} \\ n_{12}^* \\ n_{21} \\ n_{22}^* \end{bmatrix}. \tag{5}$$

This equation is of the form

$$Y = \boldsymbol{H}X + n \tag{6}$$

where $\boldsymbol{H}$ is the channel matrix given by

$$\boldsymbol{H} = \begin{bmatrix} h_{11} & h_{12} \\ h_{12}^* & -h_{11}^* \\ h_{21} & h_{22} \\ h_{22}^* & -h_{21}^* \end{bmatrix} \tag{7}$$

Since the two columns of the channel matrix are orthogonal, the system equation in (5) can be decoded to obtain the estimates of the transmitted signals by multiplying through by the Hermitian transpose of the channel matrix given as

$$\boldsymbol{H}^H = \begin{bmatrix} h_{11}^* & h_{12} & h_{21}^* & h_{22} \\ h_{12}^* & -h_{11} & h_{22}^* & -h_{21} \end{bmatrix} \tag{8}$$

The transmitted signals are then estimated using the equation

$$\hat{X} = \begin{bmatrix} \hat{X}_1 \\ \hat{X}_2 \end{bmatrix} = \frac{\boldsymbol{H}^H Y}{|h_{11}|^2 + |h_{12}|^2 + |h_{21}|^2 + |h_{22}|^2} \tag{9}$$

B. Space-Time Block-Coded MIMO-OFDM System

A 2×2 MIMO-OFDM system employing space-time coding is simply an extension of the 2×2 MIMO system in Fig. 1 where the blocks of OFDM signal processing are added after the STBC encoder as illustrated in Fig. 2. The

main OFDM signal-processing blocks in the transmitter are Inverse Fast Fourier Transform (IFFT), Cyclic Prefix (CP) addition, Digital-to-Analogue Converter (DAC), HPA, and RF front-end up-converter.

In the receiver section, the signal processing operations in the transmitter section are reversed. Therefore, each branch of a 2×2 MIMO-OFDM system is the same and experiences similar effects of high PAPR as a SISO-OFDM system.

C. PAPR in MIMO-OFDM System

With the consideration that each branch of a MIMO-OFDM system is equivalent to a SISO-OFDM system, the IFFT output during one-symbol duration is the baseband signal given by

$$x_i(n) = \frac{1}{\sqrt{N}} \sum_{k=0}^{N-1} X_i(k)\, e^{\frac{j2\pi kn}{N}} \tag{10}$$

Here, $X_i(k)$ is the modulation symbol from binary phase-shift keying (BPSK) or M-ary quadrature amplitude modulation (M-QAM), N is the total number of subcarriers, and $i = 1$ or 2 is the branch index.

For each branch signal $x_i(n)$, the ratio of the peak power to the average power is given by

$$\text{PAPR}\{x_i(n)\} = \frac{\max\limits_{0 \le n \le N-1} \{|x_i(n)|^2\}}{E\{|x_i(n)|^2\}} \tag{11}$$

where $\text{E}\{.\}$ is the expectation operator. For the MIMO-OFDM system, we are interested with the maximum PAPR among all branches, which for the 2×2 system is given by

$$PAPR_{MIMO} = \max(\text{PAPR}\{x_1(n)\}, \text{PAPR}\{x_2(n)\}) \tag{12}$$

Because the input to the HPA is a continuous-time signal $x_i(t)$, in the calculation of PAPR, signal $x_i(n)$ should be oversampled with a factor ≥ 4. This avoids skipping the peak value of the continuous-time signal [24] and in turn helps to closely estimate the continuous-time PAPR.

From (10), it is clear that each branch signal is a summation of N signals and therefore can have large amplitude fluctuations resulting from constructive and destructive additions. These amplitude fluctuations can result into high PAPR and nonlinear amplification effects

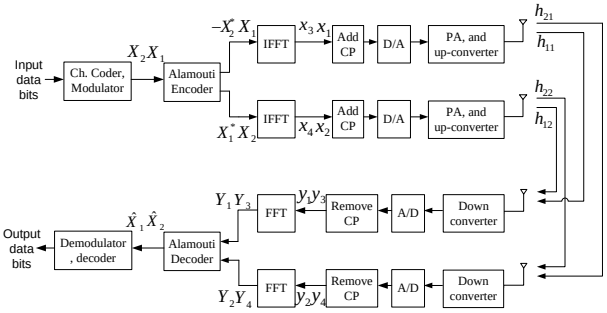

Fig. 2. MIMO-OFDM system deploying 2×2 Alamouti STBC.

when the signal is passed through the HPA. Analytically, the distribution of the magnitudes of the amplitudes, i.e. $|x_i(n)|$, can point as to whether or not a signal has high power fluctuations and therefore high PAPR.

Assuming a sufficiently large N and that the signal amplitudes are statistically independent and identically distributed, by the central limit theorem, both the real and imaginary parts of the amplitudes are Gaussian-distributed and therefore the signal magnitudes $|x_i(n)|$ are Rayleigh-distributed. Consequently, signal $x_i(n)$ can have high PAPR. The highness of a PAPR can be measured using the complementary cumulative distribution function (CCDF), which is the probability that PAPR is above a given threshold γ and is given by the equation

$$\Pr\{\text{PAPR}\{x_i(n)\} > \gamma\} = 1 - (1 - e^{-\gamma})^N \tag{13}$$

where $\Pr\{.\}$ is the probability operator.

From (13), for fixed values of CCDF and N, a high value of threshold indicates a high PAPR and vice versa. This has the interpretation that for a given CCDF value, the difference between any two-threshold values can be used as a measure of PAPR reduction and to indicate how well any proposed method reduces PAPR.

III. Proposed Method

In this paper, we propose a low-complexity method that reduces PAPR in MIMO-OFDM systems by generating additive peak-cancelling signals to reduce high signal amplitudes in transmitted signals. The proposed method is referred to as "low-complexity additive signal mixing" or in short form ASM PAPR reduction method. In order to avoid BER degradation due to clipping of high signal amplitudes, a few samples of the peak-cancelling signals are appended to the transmitted signals for the restoration of clipped amplitudes at the receiver. The peak-cancelling signals are derived from MIMO-OFDM transmit signals considering the peak power that the HPA can handle without signal distortion.

A. Proposed Algorithm

For exact cancellation of the highest peaks in a transmit signal without introducing new ones, a peak-cancelling signal should only have samples of signal peaks exceeding a clipping threshold. The clipping threshold can generally be set based on the desired PAPR level in a system. For a given clipping threshold x_{th}, the desired peak-cancelling signal for signal $x_i(n)$ can be generated according to the equation

$$d_i(n) = \begin{cases} \dfrac{x_i(n)}{|x_i(n)|}(|x_i(n)| - x_{th}), & |x_i(n)| > x_{th} \\ 0 \qquad\qquad\qquad\quad , & |x_i(n)| \le x_{th} \end{cases} \tag{14}$$

In vector form this signal can be expressed as $\boldsymbol{d}_i = [d_i(0), d_i(1), \ldots, d_i(N-1)]^T$. The signal has both zero and nonzero samples. A simplified discrete-time signal $c_i(k)$ containing only the nonzero entries can be written as

$$\boldsymbol{c}_i = [c_i(0), c_i(1), \dots, c_i(M-1)]^T \quad (15)$$

where M is the number of nonzero samples in $d_i(n)$.

The tone reservation concept in [25] can be used to generate a peak-cancelling signal that estimates the signal in (14). This can be accomplished by reserving L subcarriers and then solving for the frequency-domain peak-cancelling coefficients from the following system of linear equations:

$$\widehat{\boldsymbol{Q}}\boldsymbol{C}_i = \boldsymbol{d}_i \quad (16)$$

where $\boldsymbol{C}_i \in \mathbb{C}^L$ is the peak-cancelling vector with L coefficients, $\widehat{\boldsymbol{Q}}_i \in \mathbb{C}^{N\times L}$ is the submatrix made up of L columns, corresponding to the locations of reserved subcarriers in the IDFT matrix $\boldsymbol{Q} \in \mathbb{C}^{N\times N}$ whose elements are given by $(1/\sqrt{N})\exp(j2\pi kn/N)$.

Due to the reservation of L subcarriers that do not carry user data, there is a loss in data rate as indicated by the following ratio:

$$R_{l,f} = \frac{L}{N} \quad (17)$$

In order to reduce the data rate loss, it is desirable to have a very low value of L that is much smaller than N but this may negatively affect the PAPR reduction capability of the tone-reservation method.

Because $L \ll N$, the system in (16) is overdetermined and can only be solved through the least-squares minimization [26]-[28] of the residual error

$$\boldsymbol{\epsilon_i} = \widehat{\boldsymbol{Q}}_i\boldsymbol{C}_i - \boldsymbol{d}_i \quad (18)$$

resulting in the closed form solution

$$\boldsymbol{C_i} = \left[\widehat{\boldsymbol{Q}}_i^H\widehat{\boldsymbol{Q}}_i\right]^{-1}\widehat{\boldsymbol{Q}}_i^H\boldsymbol{d}_i \quad (19)$$

After finding the frequency-domain coefficients, the time-domain peak-cancelling signal is obtained using the equation

$$\widehat{\boldsymbol{d}}_i = \widehat{\boldsymbol{Q}}_i\boldsymbol{C}_i \quad (20)$$

and the PAPR-reduced signal is then given by

$$s_i(n) = x_i(n) - \hat{d}_i(n) \quad (21)$$

Because of the over-deterministic nature of the system determining the peak-cancelling coefficients, the peak-cancelling signal $\widehat{\boldsymbol{d}}_i$ cannot be equal to the desired signal $\boldsymbol{d}_i$, and has nonzero elements even in positions that had zeros in the desired signal. This can lead to the generation of new signal peaks in the PAPR-reduced signal $s_i(n)$ and in turn result in poor PAPR reduction. The only way to improve the solution in (19), in order to have $\widehat{\boldsymbol{d}}_i \cong \boldsymbol{d}_i$, is to sufficiently increase L towards N but this will lead to an unacceptably high data rate loss.

Therefore, the two requirements of high PAPR reduction and low data rate loss compete directly with each other, and this poses a design dilemma in the development of the PAPR reduction method. In order to achieve both a high PAPR reduction and a minimum data rate loss, we propose, in this work, an algorithm that directly employs the desired peak-cancelling signal in (14) to reduce PAPR. The PAPR-reduced signal in this case is given by

$$s_i(n) = x_i(n) - d_i(n) \quad (22)$$

This ensures that all the highest speaks of the signal $x_i(n)$ are cancelled out without generating new ones. However, the clipping of the signal amplitudes will result in BER degradation. To avoid this, a few samples, the nonzero ones, of the desired peak-cancelling signal will be transmitted together with the PAPR-reduced signal to enable the receiver reconstruct back the clipped amplitudes.

However, the transmission of the nonzero peak-cancelling samples affects the system data rate because they do not carry user data. This data rate loss occurs in the time-domain and is given by

$$R_{l,t} = \frac{M}{N+M}. \quad (23)$$

But for the same number of reserved tones and nonzero time samples, the data rate loss in the proposed method is less than the one given in (17) for the tone-reservation based methods. However, owing to the choice of the clipping threshold, which must be greater than the average value of the signal, the number of nonzero samples in $d_i(n)$ will be in all cases very small compared to the length of the signal i.e. $M \ll N$ and therefore $R_{l,t} \approx 0$.

Logically, the threshold at which signal $x_i(n)$ is clipped can be expressed as a function of the average value of the signal using the equation:

$$x_{th} = \lambda\mu \quad (24)$$

where μ is the mean of the signal amplitudes $|x_i(n)|$, and λ is the threshold adjustment parameter in the range $1 < \lambda < \max(|x_i(n)|)/\mu$.

When for a given system, the maximum allowed PAPR is known, the required x_{th}, and hence λ, can be found directly from equation (12). After the determination of the clipping threshold, M can be obtained analytically from the distribution of the signal amplitudes. For such a derivation, let X_n denote a Rayleigh random variable representing the distribution of the signal amplitudes that is given by the equation

$$F_{X_n}(x) = 1 - e^{-\frac{x^2}{2\sigma^2}}, \quad x \geq 0 \quad (25)$$

where σ is the scaling parameter of the distribution. The average value of the distribution is

$$\mu = \sigma\sqrt{\frac{\pi}{2}} \quad (26)$$

From (25), the probability of signal amplitude being greater than the clipping threshold is given by:

$$P(X_n > x_{th}) = e^{-\frac{{x_{th}}^2}{2\sigma^2}} \tag{27}$$

and since this is equal to the ratio M/N, then by substituting (24) in (27), the number of nonzero entries in $d_i(n)$ is obtained as follows:

$$M = Ne^{-\frac{\pi}{4}\lambda^2} \tag{28}$$

Equation (28) indicates that the number of nonzero elements in the peak-cancelling signal decreases exponentially with the clipping threshold. The maximum value of M will occur in the trivial case when the clipping threshold is equal to the average value, corresponding to $\lambda = 1$ and $M = 0.46N$. The minimum value of M will occur when $x_{th} = \max(|x_i(n)|)$. Then, in all practical cases, $M \ll N$ and therefore the data rate loss will always be negligible.

The proposed algorithm is flexible in terms of the inputs it can use to process peak-cancelling signals from original transmit signals. Either it can use the maximum acceptable PAPR or the maximum allowed data rate loss. When one of either of the two inputs is given, the algorithm can compute the other and determine whether it is within the acceptable limits. If M or the maximum allowed data rate loss is known, by using (28) the clipping threshold can be obtained as follows:

$$x_{th} = \mu\sqrt{\frac{4}{\pi}\ln\left(\frac{N}{M}\right)} \tag{29}$$

After obtaining x_{th}, the peak-cancelling signal can be found from (14).

Fig. 3 shows two typical peak-cancelling signals for a 2×2 MIMO-OFDM system. It can be observed that for the second transmit antenna, the peak-cancelling signal has 13 nonzero samples while in the first antenna signal they are 10. The highest peak also occurs in the second antenna signal. Consequently, this means that a higher PAPR reduction is required on the transmit signal from the second antenna than on the one from the first antenna. Additionally, because of the oversampling by a factor of 4, N is equal to 1024/4 = 256 and the data rate loss $R_{l,t} = 0.048$.

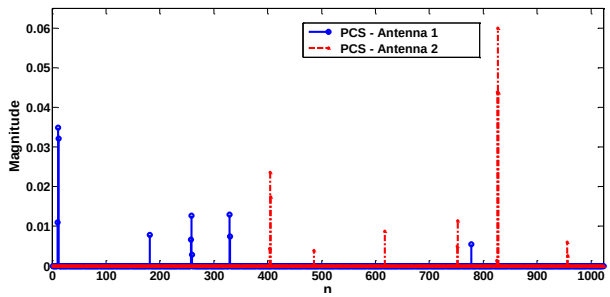

Fig. 3. Peak-cancelling signals in 2 × 2 MIMO-OFDM system.

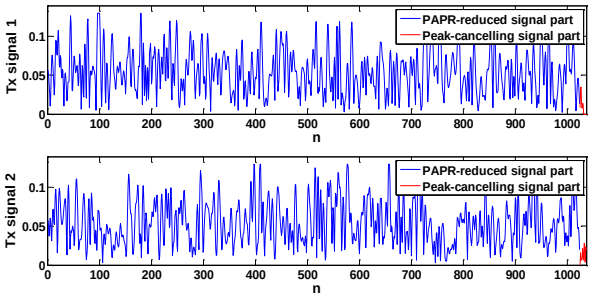

Fig. 4. Composite transmit signals in 2×2 MIMO-OFDM system.

The corresponding composite signals from the two transmit antennas are shown in Fig. 4. From this figure, it is evident that when $M \ll N$ the waveform of the PAPR-reduced signal is barely affected by the addition of M peak-cancelling signal samples. Intuitively, this also means that the transmission of the M samples has no significant effect on the average transmit power.

However, analytically, the effect of transmitting the nonzero peak-cancelling samples on the average transmit power can be established by considering the sum of the powers in the clipped samples and the peak-cancelling clipped samples. For this purpose, let $\tilde{x}_i(k)$ denote the set of non-clipped samples greater than the clipping threshold x_{th} in the i^{th} branch signal $x_i(n)$ in the MIMO-OFDM system. After the amplitude-clipping of the signal $x_i(n)$, all the samples in $\tilde{x}_i(k)$ will have the same signal magnitude equal to x_{th}. Since all the signal magnitudes $|x_i(n)|$ are in the range of 0 to 1, the sum of the powers in the clipped and peak-cancelling samples will always be less than or equal to the total power in the original non-clipped samples i.e.

$$\sum_{k=1}^{M}(x_{th}^2 + |c_i(k)|^2) \leq \sum_{k=1}^{M}|\tilde{x}_i(k)|^2 \tag{30}$$

Equation (30) may suggest that the power of the composite signal can decrease with the number of nonzero samples. However, again, because of the range of values occupied by the signal amplitudes, such power reductions are very small. Therefore, the power of the original transmit signal is practically maintained by the proposed method.

From the foregoing description, the proposed algorithm can be summarized as follows:

ASM Algorithm

i. Set the number of subcarriers N, data rate loss $R_{l,t}$, and $PAPR_{max}$
ii. Generate MIMO-OFDM signals $x_i(n)$, $i = 1,2, \ldots N_t$
iii. Find $PAPR_{MIMO}$
iv. If $PAPR_{MIMO} < PAPR_{max}$, transmit $x_i(n)$ and terminate the algorithm, else go to step (v)
v. Set clipping threshold x_{th}
vi. Generate desired peak-cancelling signals $d_i(n)$
vii. Generate peak-reduced signals $s_i(n) = x_i(n) - d_i(n)$
viii. Determine nonzero samples in $d_i(n)$ and generate signals $c_i(k)$

ix. Append $c_i(k)$ to $s_i(n)$ and transmit combined signal
x. End

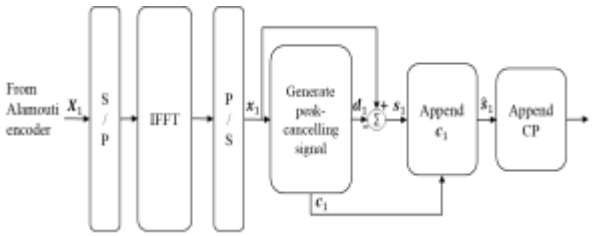

Fig. 5. Transmitter section integrating ASM method.

A MIMO-OFDM system integrating the proposed PAPR reduction is illustrated in Fig. 5. The illustration is for one of the MIMO branches during the first symbol duration. The OFDM symbol $\boldsymbol{X}_1$ from the Alamouti encoder is first converted from serial to parallel (S/P) format and then passed to the IFFT to obtain a time-domain signal, which is then converted back to serial format to produce signal $\boldsymbol{x}_1$. The proposed method is then applied to $\boldsymbol{x}_1$ to produce two outputs: the peak-cancelling signal $\boldsymbol{d}_1$ and its compressed version $\boldsymbol{c}_1$ containing only the nonzero samples. Signal $\boldsymbol{d}_1$ is then subtracted from $\boldsymbol{x}_1$ to get a PAPR-reduced signal $\boldsymbol{s}_1$, which is then extended by $\boldsymbol{c}_1$ to yield the composite transmit signal $\hat{\boldsymbol{s}}_1$.

The composite transmit signal is then cyclically extended in the append CP block with a cyclic prefix of length greater than the expected channel duration. The extension is realized by copying some samples at the tail end of the signal to the front end to provide a time guard interval for the elimination of the ISI. After the CP addition, the composite transmit signal is amplified through the HPA and then passed on for RF transmission.

At the receiver, after removing the cyclic prefix, the M peak-cancelling samples in $\boldsymbol{c}_1$ are also removed and added back to the clipped samples to reconstruct the original OFDM signal $\boldsymbol{x}_1$, which is then passed to the FFT block for demodulation and after decoded into binary data.

B. High Power Amplifier Modelling

The Rapp model [29] of the HPA is used in this work. The model has a constant AM/PM characteristic, which makes it suitable for modelling the phase distortion of the solid-state power amplifier (SSPA). On the other hand, the AM/AM characteristic of the model can be easily tuned to simulate various nonlinear characteristics of the HPA. In the model, it is assumed that the HPA has a linear performance up to a point near the saturation point. Near the saturation point, a transition towards a constant saturated output is applied on the input signal.

Since the model does not introduce any phase distortions, the AM/PM relation can be written as

$$\varphi(x(n)) \approx 0 \tag{31}$$

This means that the HPA does not introduce any phase changes during the amplification of the input signal.

For the amplitude amplification, the general expression for the AM/AM conversion is given by

$$g(x(n)) = \frac{x(n)}{\left(1 + \left(\frac{|x(n)|}{A_{sat}}\right)^{2p}\right)^{\frac{1}{2p}}} \tag{32}$$

Here, $x(n)$ is the input signal and A_{sat} denotes the output at the 3-dB point and is used to set the HPA saturation level. The smoothness parameter p is used to smoothen the amplification during the transition from the linear to the saturation region. Therefore, a smaller p means a smoother transition and vice versa.

C. Computational Complexity

The proposed algorithm performs two main operations, which are the generation of peak-cancelling signal using (14) and the signal addition operation in (22) to reduce PAPR. The operation of computing the peak-cancelling signal requires $2M$ real multiplications and $2M$ real additions while the operation for reducing PAPR requires $2M$ real additions. At the receiver, the reconstruction of the clipped signals peaks requires $2M$ real additions.

The multiplication operations are more computationally intensive than the additions and are the one that determines the overall complexity of an algorithm. Therefore, in the order of the number of multiplications, the computational complexity of the proposed method is $O(M)$.

Because the main part of the proposed method is to be implemented in the transmitter and therefore form part of the signal processing, there is need to consider any arising increase in the overall computational complexity. For the OFDM signal processing at the transmitter, the most complex operation is the IFFT, which has a computational complexity of $O(N \log_2 N)$. Since $M \ll N$, then $O(M) \lll O(N \log_2 N)$. This means that incorporating the proposed method into a MIMO-OFDM system will not change the overall computational complexity of the system.

IV. Results and Discussion

The proposed ASM PAPR reduction method was applied to reduce PAPR in MIMO-OFDM systems. Simulations of MIMO-OFDM systems were carried out in MATLAB. The key simulation parameters are listed in Table I. An Alamouti space-time code was used with 2 transmit and 2 receiver antennas over Rayleigh flat-fading channels. The Rapp model of the HPA was used in the simulations. In each simulation scenario, the proposed algorithm was executed for 10^4 symbols.

Table I: Simulation Parameters

FFT window size	128, 256
Modulation	QPSK
Number of OFDM symbols	10^4
Oversampling factor F_s	4
Power amplifier model	Rapp model, p = 2
Guard interval	1/4
Channel model	Rayleigh flat-fading

As it is indicated in the table, all the subcarriers were modulated with QPSK data. This is sufficient for ascertaining the method's performance and for comparison to other methods because the type of modulation does not affect the PAPR reduction performance. Both the PAPR reduction and the BER performances were analysed.

The very first simulations were to help assess the PAPR reduction capability of the proposed method. For this task, a system with $N = 256$ subcarriers was employed. The system was subjected to the following number of peak-cancelling samples: $M = 3$, 6, 13, 19, and 26. These values of M correspond to the following data-rate losses: 1.2%, 2.3%, 4.8%, 6.9%, and 9.2%, respectively. The reduction of PAPR was then evaluated for each case using the CCDF as shown in Fig. 6.

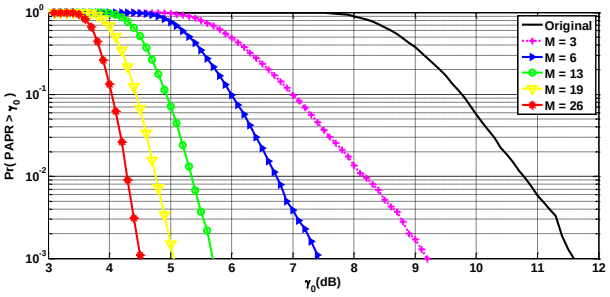

Fig. 6. CCDF for MIMO-OFDM system with QPSK data and N = 256.

TABLE II: PAPR REDUCTIONS AT CCDF = 10^{-3}, N = 256

M	3	6	13	19	26
$R_{l,t}$ (%)	1.2	2.3	4.8	6.9	9.2
PAPR Reduction (dB)	2.4	4.2	5.9	6.5	7.1
Power Change (dB)	-0.02	-0.04	-0.09	-0.13	-0.18

In Table II, the results for PAPR reductions at CCDF $= 10^{-3}$ and transmit power changes due to the use of different number of peak-cancelling samples are given. From this table, it is evident that the capability of the proposed method to reduce PAPR depends on the number of the peak-cancelling samples employed. However, it can also be observed that with only a small number of peak-cancelling samples, high PAPR reductions can be achieved e.g. with only 6 samples a good reduction of 4.2 dB could be achieved.

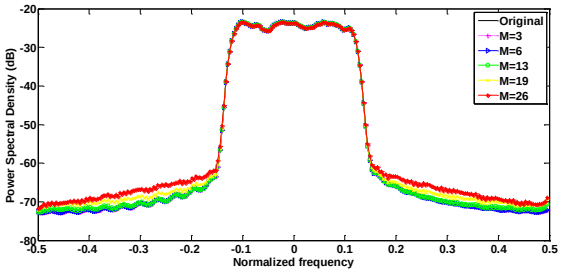

Fig. 7. Power spectral densities for different PAPR-reduced signals.

In addition, on the tabulated results for the average power it is clear that the transmit power of the signal is practically maintained before and after PAPR reduction. For example, for M = 26, the average transmit power is 99.3% of the value before the PAPR reduction. Moreover, from the power spectral densities plots in Fig. 7, it can be observed that due to the small amount of clipping on only a few number of signal amplitudes, the out-of-band radiations are negligible.

After ascertaining the ability of the proposed ASM method to reduce PAPR, it was then compared with four other promising PAPR reduction methods proposed in literature, which were earlier on given the acronyms SCS-SLM, STR, ACT and CSC. For the purpose of this comparison, a MIMO-OFDM system with QPSK-modulated subcarriers and $M = 23$ samples, equivalent to a data rate loss of 15%, was used. The results showing the PAPR reduction performances of the different methods are shown in Fig. 8 and also given in Table III for CCDF $= 10^{-3}$.

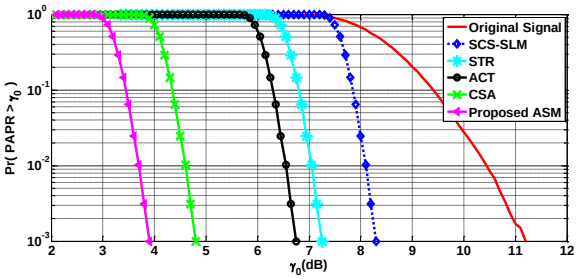

Fig. 8. PAPR reduction by different methods, N = 128.

Apparently, the proposed method shows better PAPR reduction capability than the other four methods and this is well demonstrated in the available results. For example, from the results in Table III, the proposed ASM method gives a PAPR reduction that is higher by 0.9, 2.85, 3.35, and 4.4 dB than the corresponding reductions by CSC, ACT, STR and SCS-SLM methods.

TABLE III: PAPR REDUCTIONS AT CCDF =10^{-3}, N = 128

Method	ASM	CSA	ACT	STR	SCS-SLM
PAPR reduction (dB)	7.30	6.40	4.45	3.95	2.90

The second simulations were used to evaluate the BER performance of MIMO-OFDM systems employing the proposed method. These tests matter a lot because BER performance is the single most important indicator of whether or not a receiver in a communication system can recover transmitted symbols. The Rapp model of HPA was used with an input power back-off (IBO) set just slightly above the PAPR value of signals at CCDF $= 10^{-3}$. This ensured that the number of symbols clipped by the HPA was less than 1%.

After amplification through the HPA, the composite signal was transmitted over Rayleigh flat-fading channels with additive white Gaussian noise. The BER degradation when using different number of nonzero peak-cancelling samples was first considered followed by a BER performance comparison with the other methods.

In Fig. 9, the BER degradations caused by the use of different values of M are shown. There are two curves labelled "Ideal": one for when the system was simulated without the use of any PAPR reduction method and HPA, and the other for the case without PAPR reduction method but with HPA backed-off by 12.5 dB—a value slightly above the maximum PAPR value of 11.8 dB at CCDF $= 10^{-3}$. The two ideal cases are similar and give the best-expected case of BER performance by the system.

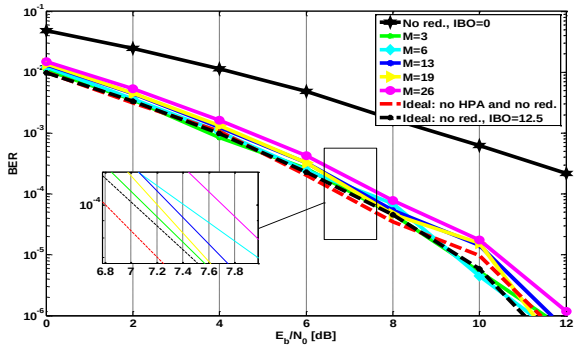

Fig. 9. BER performance by different M-values, N = 256.

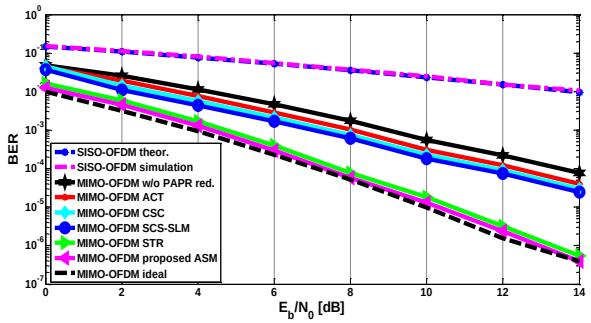

Fig. 10. BER performance by different methods, N = 128.

The worst expected BER performance is given by the curve labelled "No red., IBO=0", which corresponds to the case when there was no PAPR reduction and the HPA was not provided with input back-off. For this case, the HPA clipped all the signal amplitudes that had power greater than the average power, and thereby highly degrading the BER.

For the other curves for the different values of M, it can be observed that the degradation of BER slightly increases with M. However, all the curves for the different values of M are tightly close to the ideal BER curves. This shows that the proposed method can effectively reduce PAPR, and thereby improving the HPA efficiency, without significantly degrading the BER performance of the MIMO-OFDM system.

For the comparison with other methods, the BER performances of the various methods are depicted in Fig. 10. In the case of SISO-OFDM system, the BER curve by theoretical formula and that by simulation are merged, thus implying the same BER performance. The simulated case had the proposed method modified and employed to reduce PAPR in the SISO-OFDM system. The curve labelled "MIMO-OFDM ideal" is the lower limit BER performance as it corresponds to the case when the HPA and PAPR reduction were not used. The curve labelled "MIMO-OFDM w/o PAPR red." is the worst-case and the upper limit performance as it corresponds to the case when no PAPR reduction method was applied to the transmit signal prior to amplification in the HPA.

As it can be observed from the BER curves, the BER performance of all the MIMO cases, even for the worst case, were by far much better than for the two SISO cases. This confirms the theory that was presented earlier that the BER falls exponentially with the diversity order. Additionally, it can be observed that both the proposed ASM method and the STR method have BER degradations close to the ideal case while the SCS-SLM, CSC, and ACT have poor performances.

In the overall, the BER performance of the proposed method is the best. For example, from the results in Table IV of the required SNR per bit, i.e. E_b/N_0, at BER = 10^{-3}, the proposed method requires an E_b/N_0 that is smaller by 0.29, 2.68, 3.05, and 3.64 dB to that needed by the STR, SCS-SLM, CSC and ACT methods, respectively.

TABLE IV: REQUIRED E_b/N_0 BY DIFFERENT METHODS AT BER = 10^{-3}

Method	**ASM**	**STR**	**SCS-SLM**	**CSC**	**ACT**
E_b/N_0 (dB)	4.36	4.75	7.04	7.41	8.00

V. CONCLUSION

In this paper, a new PAPR reduction method for MIMO-OFDM systems has been proposed. The method utilizes a low-complexity additive signal-mixing concept to reduce PAPR by first designing a peak-cancelling signal for each MIMO diversity arm, and then adding it to each arm's transmit signal. To avoid BER degradation due to peak reductions, a few samples of the peak-cancelling signal are appended to the transmit signal to be used for amplitude reconstructions at the receiver.

Therefore, the method reserves peak-cancelling resources in the time domain rather than in the frequency domain. This makes the method to have a lower data rate loss than in a conventional tone reservation method that reserves peak-cancelling resources in the frequency domain.

An investigation into PAPR reduction capability showed that the proposed method could achieve significant PAPR reductions with very low data rate losses while practically maintaining average transmission powers of original MIMO-OFDM signals. In addition, the method has a low computational complexity of $O(M)$, which is by far much less than the FFT complexity of $O(N \log_2 N)$.

Additionally, the method does not degrade the BER of the initial MIMO-OFDM system. In overall, in comparison with four other PAPR reduction methods: ACT, STR, SCS-SLM and CSC, the proposed method gives better PAPR reduction and BER performances.

CONFLICT OF INTEREST

The authors declare no conflict of interest.

AUTHOR CONTRIBUTIONS

Stephen Kiambi conducted the research, analyzed the data and wrote the paper. Elijah Mwangi and George Kamucha reviewed and corrected the paper. All authors approved the final version of the paper.

REFERENCES

[1] Y. Cho, J. Kim, W. Yang, and C. Kang, *MIMO-OFDM Wireless Communications with MATLAB*, John Wiley & Sons (Asia) Pte Ltd, Singapore, 2010.

[2] Y. Rahmatallah and S. Mohan, "Peak-to-average power ratio reduction in OFDM systems: A survey and taxonomy," *IEEE Comm. Surveys and Tutorials*, vol. 15, no. 4, pp. 1567-1592, 2013.

[3] Y. Louët and J. Palicot, "A classification of methods for efficient power amplification of signals," *Annals of Telecom.*, vol. 63, no. 7-8, pp. 351-368, 2008,.

[4] J. Armstrong, "Peak-to-average power reduction for OFDM by repeated clipping and frequency domain filtering," *IEE Electronic Lett* , pp. 246–247, 2002.

[5] R. Zayani, H. Shaiek, and D. Roviras, "PAPR-aware massive MIMO-OFDM downlink," *IEEE Access*, vol. 7, pp. 25474-25484, 2019.

[6] Vallavaraj, B. G. Stewart, and D. K. Harrison, "An evaluation of modified μ-law companding to reduce the PAPR of OFDM systems," *AEU-Int. J. Electron. Commun*., vol. 64, no. 9, pp. 844-857, 2010.

[7] H. B. Jeon, J. S. No, and D. J. Shin, "A low-complexity SLM scheme using additive mapping sequences for PAPR reduction of OFDM signals," *IEEE Trans. Broadcast.*, vol. 57, no. 4, pp. 866-875, 2011.

[8] T. Jiang, C. Ni, and L. Guan, "A novel phase offset SLM scheme for PAPR reduction in alamouti MIMO-OFDM systems without side information," *IEEE Signal Process. Lett.*, vol. 20, no. 4, pp. 383-386, 2013.

[9] Lahcen, A. Saida, and A. Adel, "Low computation complexity PTS scheme for PAPR reduction of MIMO-OFDM systems," in *Proc. 10th Int. Conf. Interdispl. in Eng., Procedia Eng.*, vol. 181, 2017, pp. 876-883.

[10] S. Kiambi, E. Mwangi, and G. Kamucha, "An iterative Re-Weighted least-squares tone reservation method for PAPR reduction in OFDM systems," *WSEAS Trans. on Comm.*, vol. 18, pp. 153–161, 2019.

[11] Ni, Y. Ma, and T. Jiang, "A novel adaptive tone reservation scheme for PAPR reduction in large-scale multiuser MIMO-OFDM systems," *IEEE Wireless Commun. Lett.*, vol. 5, no. 5, pp. 480-483, 2016.

[12] Tang, K. Qin, and H. Mei "A hybrid approach to reduce the PAPR of OFDM signals using clipping and companding," *IEEE Access*, vol. 8, pp. 18984-18994, 2020.

[13] B. Bakkas, I. Chana, and H. Ben-Azza, "PAPR reduction in MIMO-OFDM based on polar codes and companding," *Proc. IEEE CommNet*, 2019, pp. 1-6.

[14] Beena, S. Pillai, and N. Vijayakumar, "Hybrid PTS-clipping scheme for PAPR reduction in MIMO-OFDM systems," *Int. Journal of Applied Eng. Research*, vol. 13, no. 11, pp. 9924-9928, 2018.

[15] Sandoval, G. Poitau, and F. Gagnon, "Hybrid peak-to-average power ratio reduction techniques: review and performance comparison," *IEEE Access*, vol. 5, pp. 27145-27161, 2017.

[16] S. Singh and A. Kumar, "Performance analysis of adaptive clipping technique for reduction of PAPR in Alamouti coded MIMO-OFDM systems," *Procedia Comp. Sci. 93*, 609 – 616, 2016.

[17] Abdullah and M. Hidayat, "SCS-SLM PAPR reduction technique in STBC MIMO-OFDM systems," in *Proc.7th IEEE ICCSCE, Penang, Malaysia*, 2017, pp. 104-109.

[18] Sandoval, G. Poitau, and F. Gagnon, "On optimizing the PAPR of OFDM signals with coding, companding, and MIMO," *IEEE Access*, vol. 7, pp. 24132-24139, 2019.

[19] B. Horvath and B. Botlik, "Optimization of tone reservation-based PAPR reduction for OFDM systems," *Radio Engineering*, vol. 26, no. 3, pp. 791-797, 2017.

[20] M. Habibi and M. Naeiny, "Selective tone reservation method for PAPR reduction in SFBC-OFDM systems," *J. of Commun. Eng.*, vol. 3, no. 2, pp. 109-122, 2014.

[21] S. Alamouti, "A simple transmit diversity technique for wireless communications," *IEEE J. Sel. Areas Commun.*, vol. 16, no. 8, pp. 1451-1458, 1998.

[22] Dahlman, S. Parkvall, J. Sköld, and P. Beming, *3G Evolution: HSPA and LTE for Mobile Broadband*, 1st ed., Elsevier Ltd, London, UK, 2007.

[23] J. Andrews, A. Ghosh, and R. Muhamed, *Fundamentals of WiMAX: Understanding Broadband Wireless Networking*, Pearson Education, Inc., USA, 2007.

[24] M. Sharif, M. Gharavi-Alkhansari, and B. H. Khalaj, "New results on the peak power of OFDM signals based on oversampling," in *Proc. IEEE ICC*, vol. 2, 2002, pp. 866–871.

[25] J. Tellado, "Peak to average power reduction for multicarrier modulation," Ph.D. dissertation, Dept. Elect. Eng., Stanford University, Stanford, CA, USA, 2000.

[26] A. Ben-Israel and T. N. E. Greville, *Generalized Inverses: Theory and Applications*, 2nd ed., Springer-Verlag, New York, 2003.

[27] R. L. Burden and J. D. Faires, *Numerical Analysis*, Brooks/Cole, Cengage Learning, 9th ed., Boston, USA, 2011.

[28] L. Xin and W. Yi, "A new weighted tone reservation method for PAPR reduction in OFDM systems," *J. of Commun.*, vol. 9, no. 12, pp. 980-986, 2014.

[29] Rapp, "Effects of HPA-nonlinearity on a 4-DPSK/OFDM-signal for a digital sound broadcasting signal," in *Proc. 2nd Eur. Conf. Satell. Commun.*, Liège, Belgium, Oct. 1991, pp. 179-184.

Stephen Kiambi received the B.Sc. degree in electrical and electronic engineering from University of Nairobi, Nairobi, Kenya, in 2000 and the M.Sc. degree in information and

communication systems from Hamburg University of Technology, Hamburg, Germany, in 2010. He is currently pursuing the Ph.D. degree in electrical and electronic engineering in the University of Nairobi, Kenya. His current research interests include signal processing in wireless and mobile communication networks, OFDM, and PAPR reduction in multicarrier systems.

Elijah Mwangi received the B.Sc. and M.Sc. degrees in electrical and electronic engineering from University of Nairobi, Nairobi, Kenya, in 1978 and 1983, respectively, and the Ph.D. degree in electrical and electronic engineering from Loughborough University of Technology, Loughborough, UK, in 1987. Since 1981, he has been with the School of Engineering, University of Nairobi, Nairobi, Kenya, where he is currently a Professor. His current research interests include digital signal processing, digital image processing, OFDM and PAPR reduction in multicarrier systems.

George Kamucha received the B.Tech. degree in electrical and communications engineering from Moi University, Eldoret, Kenya, in 1990, M.Sc. degree in biomedical engineering from University of Aberdeen, Aberdeen, UK, in 1994, and the Ph.D. degree in electrical engineering from University of Kassel, Kassel, Germany, in 2003. Since 2010, he has been with the School of Engineering, University of Nairobi, Nairobi, Kenya, where he is currently a Senior Lecturer. His current research interests are in biomedical and communication systems.